Spin Controlling in Narrow Zigzag Silicon Carbon Nanoribbons by Carrier Doping

Ping Lou*,†,‡ and Jin Yong Lee*,†

Department of Chemistry, Sungkyunkwan University, Suwon 440-746, Korea, and Department of Physics, Anhui University, Hefei 230039, Anhui, China

Received: December 17, 2009; Revised Manuscript Received: March 21, 2010

By means of first-principles calculations we predict that it is possible to manipulate the magnetization and magnetization direction in narrow zigzag silicon carbon nanoribbons (ZSiC NRs) by carrier (hole and electron) doping. Without doping, the ground state of the ZSiC NRs wider than 0.6 nm is ferrimagnetic with local magnetic moments at the edge atoms C and Si that are passivated by the hydrogen atoms, and their orientations are parallel at each zigzag edge and are antiparallel between the two edges. Consequently, the magnetic moment per cell of the ZSiC NR is almost zero. It is found that the hole doping enhances the local magnetic moment at the edge C atoms, but weakens the local magnetic moment at the edge Si atoms. As a result, the ZSiC NR is *magnetized*, and the magnetization direction conforms to the local magnetic moment at the edge C atoms. In contrast, the electron doping weakens the local magnetic moment at the edge C atoms, while it enhances the local magnetic moment at the edge Si atoms. As a result, the ZSiC NR is also *magnetized*, and the magnetization direction conforms to the local magnetic moment at the edge Si atoms. Thus, the magnetization direction of the ZSiC NRs depends on the type of carrier doping.

Introduction

Spintronic devices are believed to be smaller, faster, and far more versatile than the conventional electronic devices, which have the following functioning scheme: (1) information is stored (written) into spins as a particular spin orientation (up or down), i.e., the *magnetization*, (2) the spins, being attached to mobile electrons, carry the information along a wire, i.e., the *spin-polarized electron transport*, and (3) the information is read at a terminal. The key feature is the control and manipulation of the "spin" of the electron, instead of its charge that is the focus of the electronics.[1] It is noted that the graphene nanoribbons (NRs) offer a possibility of achieving these purposes.[2−7] Hence, the graphene NRs have attracted a lot of study.[8−45] The graphene NRs are made by cutting the graphene sheets, where the edge carbon atoms are passivated by hydrogen. It was found that the graphene NRs can be either metallic or semiconducting depending on the width and structure of the edges.[8−18] Notably, the zigzag graphene NRs (graphene nanoribbons with zigzag edges) are a magnetic semiconductor with a small band gap, and have ferromagnetic ordering at each edge and their spins at each edge are antiparallel.[16,19−28] When a very strong transverse electric field is applied, the ZG NRs transform to half metal,[19−22] where only one of the spin channels conducts, while the other remains insulating, which suggests possibilities for the control and manipulation of the *spin-polarized electron transport* by applying electric field.

However, an easy way to control the spin polarized electrons in downscaling devices has proved to be quite a challenge. It has proven elusive to manipulate the *magnetization* by applying electric field.[46,47] We recently reported that the zigzag silicon carbon nanoribbons (ZSiC NRs) can be utilized for manipulating the *magnetization* by applying an electric field.[48,49] It is found that the ZSiC NRs showed the *magnetization* by a transverse electric field as well as the conversion of spin polarization. Here, we propose another simple way to control the magnetization and magnetization direction of the ZSiC NRs by carrier (hole and electron) doping. We find that holes and electrons injected by removing or adding electrons from the ZSiC NRs result in the magnetization and change of the magnetization direction of the ZSiC NRs.

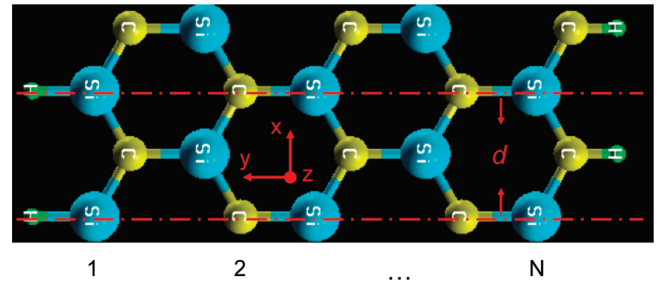

Figure 1. Geometric structure of the ZSiC NR. ZSiC NR is periodic along the *x* direction. The 1D unit cell distance and the ribbon width are denoted by *d* and *N*, respectively. The large, middle, and small spheres denote Si, C, and H atomes, respectively.

Models and Methods

In our model, *N*-ZSiC NRs is flat in the *x*−*y* plan, with *N*-zigzag chains along the *x* direction. The edges of ZSiC NRs are saturated by hydrogen atoms. Periodic boundary condition (PBC) is used to consider ZSiC NRs with infinite length, which is shown in Figure 1. Our calculations were carried out with the OPENMX computer code.[50] The DFT within the GGA[51] for the exchange-correlation energy was adopted. Norm-conserving Kleinman−Bylander pseudopotentials[52] were employed, and the wave functions were expanded by a linear combination of multiple pseudoatomic orbitals (LCPAO)[53,54] with a kinetic energy cutoff of 250 Ry. The basis functions used were as follows: C6.0-$s^2p^2d^1$, Si6.0-$s^2p^2d^1$, and H4.5-s^1p^1. The first symbol designates the chemical name, followed by the

* To whom correspondence should be addressed. E-mail: jinylee@skku.edu (J.Y.L.) and loup@ahu.edu.cn (P.L.).
† Sungkyunkwan University.
‡ Anhui University.

10.1021/jp911953z
Published on Web 05/28/2010

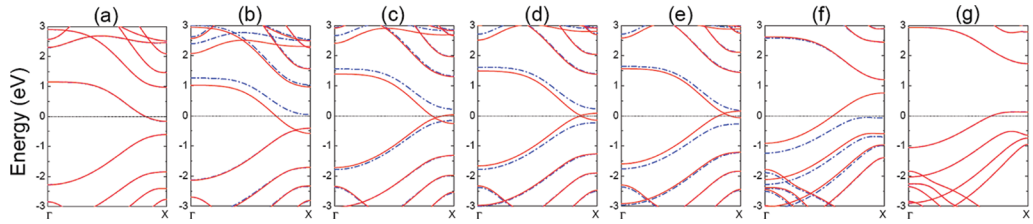

Figure 2. Band structures and corresponding spatial distribution of the spin differences of 4-ZSiC NR in the ground state with x electrons added or removed per unit cell ($x = 0$ for undoping, $x < 0$ for electron doping, and $x > 0$ for hole doping). Panels a, b, c, d, e, f, and g show the results for $x = -0.35$, -0.3, -0.1, 0, 0.1, 0.45, and 0.6, respectively. For the band structures, the red solid and blue dash-dotted lines denote the spin-up and spin-down bands, respectively. The Fermi level is set to zero.

cutoff radius (in Bohr radius) in the confinement scheme, and the last set of symbols defines the primitive orbitals applied. We adopted a supercell geometry (Figure 1) where the length of a vacuum region along the nonperiodic direction (y-, z-directions) was 20 Å, and the lattice constant along the periodic direction (x-direction) was 3.11 Å. Previously, it was suggested that enough k-point sampling in the Brillouin zone integration should be performed for reliable results (see Figures S8, S9, and S10 in the Supporting Information).[49,55] Thus, we used 120 × 1 × 1 k -point sampling points in the Brillouin zone integration. The geometries were optimized until the Hellmann−Feynman forces were less than 10^{-4} hartree/bohr. The convergence in energy was 10^{-8} hartree. We have also increased the size of the supercell to make sure that it does not produce any discernible difference on the results. Holes and electrons doping were performed by a shift in the Fermi level and a uniform background charge is introduced to balance the charge neutrality of the system, which is called the Fermi-level shift (FLS) method.

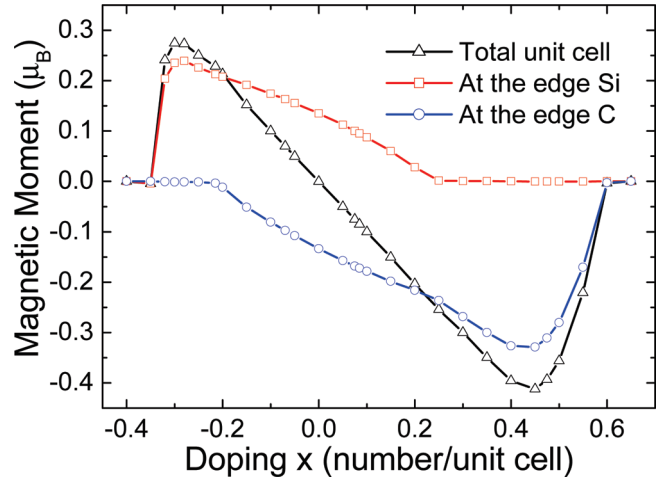

Figure 3. Magnetic moments of the total unit cell and at the edge Si and C of 4-ZSiC NR in the ground state as a function of the doping concentration x per unit cell ($x = 0$ for undoping, $x < 0$ for electron doping, and $n > 0$ for hole doping).

Results and Discussion

Figure 2 shows the band structures of 4-ZSiC NR in the ground state with x electrons added or removed per unit cell ($x = 0$ for undoping, $x < 0$ for electron doping, and $x > 0$ for hole doping). In general, for the band structures, as shown in Figure 2d, without doping ($x = 0$), the 4-ZSiC NR is a ferrimagnetic semiconductor with two different direct band gaps for the spin-up and the spin-down channels near the X point.[49] By a little carrier doping, the 4-ZSiC NR turns into ferrimagnetic metal as shown in Figure 2c,e. By large carrier doping, the 4-ZSiC NR turns into nonmagnetic metal as shown in Figure 2a,g. We also noted the difference in the spin property by doping. As shown in Figure 2d, without doping ($x = 0$), the 4-ZSiC NR has local magnetic moments at the edge C and Si atoms, and their orientations are parallel at each zigzag edge and are antiparallel between the two edges. Consequently, the magnetic moment per cell of the ZSiC NR is almost zero, 0.00043 μ_B.[49] When the hole is doped, the local magnetic moment at the edge C atoms is enhanced, while the local magnetic moment at the edge Si atoms is weakened as clearly seen in Figure 3. As a result, the ZSiC NR has been *magnetized* by hole doping! It is noted that the magnetization direction is spin-down, and the total magnetic moment conforms to the local magnetic moment at the edge C atoms. When $x \simeq 0.25$, the local magnetic moment at the edge Si atoms drops to zero, while the local magnetic moment at the edge C atoms is significantly enhanced. At $x \simeq 0.45$ (called the upper critical concentration of hole doping and expressed by x_h^{up}), the local magnetic moment at the edge C atoms reaches the maximum. After that, the local magnetic moment at the edge C atoms becomes weakened and drops to zero at $x \simeq 0.6$ (called the down critical concentration of hole doping and expressed by x_h^{down}).

On the other hand, when the electron doping is applied, the local magnetic moment at the edge C atoms is weakened, while the local magnetic moment at the edge Si atoms is enhanced. As a result, the ZSiC NR can also be magnetized by electron doping! Moreover, by electron doping, we note that not only the ZSiC NR has been *magnetized* but also the magnetization direction has been changed, i.e., the magnetization direction is converted to spin-up from spin-down. The total magnetic moment conforms to the local magnetic moment at the edge Si atoms. When $x \simeq -0.20$, the local magnetic moment at the edge C atoms drops to zero, while the local magnetic moment at the edge Si atoms is enhanced. At $x \simeq -0.3$ (called the upper critical concentration of electron doping and expressed by x_e^{up}), the local magnetic moment at the edge Si atoms reaches the maximum. By further doping, the local magnetic moment at the edge Si atoms becomes weakened and drops to zero at $x \simeq -0.35$ (called the down critical concentration of electron doping and expressed by x_e^{down}). These novel phenomena demonstrate the possibility of tuning the local magnetic moment at the edge C and Si atoms of the ZSiC NRs as well as the magnetization and the magnetization direction by doping!

The above results can be understood by the following analysis. As shown in Figure 4, without doping, the valence edge states with up spin are localized at the edge Si, while those with down spin are localized at the edge C. However, the conduction edge states show the opposite behavior. Theoretically, the carrier doping of ZSiC NR is simulated either by removing electrons from the filled spin-polarized bands, i.e., hole doping, or by adding electrons to the empty spin-polarized bands, i.e., electron doping. Thus, with hole doping, the hole will attract the electron from the valence edge states with up

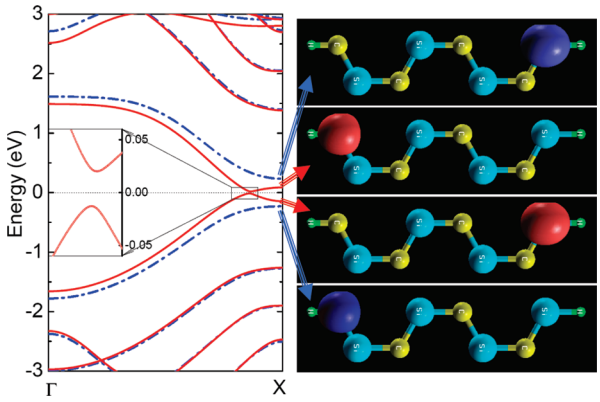

Figure 4. Band structures of 4-ZSiC NR in the ground state, and the charge densities of the highest occupied and the lowest unoccupied states at the *X* point for the spin-up (red-solid) and spin-down channels (blue-solid), respectively.

spin, which makes the spin-up channel of the valence band partially filled, while keeping the spin-down channel in this band fully occupied (see Figure 2e,f). In contrast, with electron doping, electrons will be added to the conduction edge states with up spin. Thus, the spin-up channel in the conduction band tends to be partially occupied. Meanwhile, the effects to the spin-down channel are much smaller and this channel remains empty (see Figure 2b,c). As a result, the local magnetic moments at the edge Si atoms and the edge C atoms drop to zero when $x \simeq 0.25$ and -0.20, respectively, as shown in Figure 3.

For 4-ZSiC NR, the calculated Voronoi and Mulliken charges on the edge Si atoms and the edge C atoms as a function of the doping concentration are plotted in Figure 5. Both the Voronoi and Mulliken charges for the edge atoms clearly show that the sum of the charges in spin-up and spin-down channels of the edge C atoms ($Q_C^{\uparrow} + Q_C^{\downarrow}$), as well as the edge Si atoms ($Q_{Si}^{\uparrow} + Q_{Si}^{\downarrow}$), monotonously decreases from the electron doping to the hole doping, although the change of the charges in spin-up channel is different from that in the spin-down channel. This shows that the hole doping is indeed removing electrons from the ZSiC NRs. However, the difference of the charges in spin-up and spin-down channels of the edge C atoms ($Q_C^{\uparrow} - Q_C^{\downarrow}$), as well as the edge Si atoms ($Q_{Si}^{\uparrow} - Q_{Si}^{\downarrow}$), does not monotonously change from the electron doping to the hole doping, which implies the different change of charges in spin-up channel and spin-down channel. Without doping ($x = 0$), for the edge C atoms, the charge in the spin-down channel ($Q_C^{\downarrow}$) is larger than that of the spin-up channel ($Q_C^{\uparrow}$), which leads to the local magnetic moment at the edge C atoms being spin-down ($Q_C^{\uparrow} - Q_C^{\downarrow} < 0$) (see the corresponding spatial distribution of the spin differences in Figure 2d). As for the edge Si atoms, the charge in the spin-up channel ($Q_{Si}^{\uparrow}$) is larger than that of the spin-down channel ($Q_{Si}^{\downarrow}$), which leads to the local magnetic moment at the edge Si atoms being spin-up ($Q_{Si}^{\uparrow} - Q_{Si}^{\downarrow} > 0$) (see Figure 2d).

It is noted for the edge C atoms that the charge in the spin-down channel ($Q_C^{\downarrow}$) increases slowly with hole doping, while the charge in the spin-up channel ($Q_C^{\uparrow}$) decreases. As a result, the local magnetic moment at the edge C atoms is enhanced. After $x \simeq 0.45$, the charge in the spin-down channel ($Q_C^{\downarrow}$) turns to decrease with doping, while the charge in the spin-up channel ($Q_C^{\uparrow}$) turns to increase. As a result, the local magnetic moment at the edge C atoms becomes weakened by further doping. At $x \simeq 0.6$, the charges in both the spin-up and spin-down channels ($Q_C^{\uparrow}$ and $Q_C^{\downarrow}$) are equal, and the local magnetic moment at the edge C atoms disappears. For the edge Si atoms, the charge in the spin-down channel ($Q_{Si}^{\downarrow}$) increases slowly with doping, while

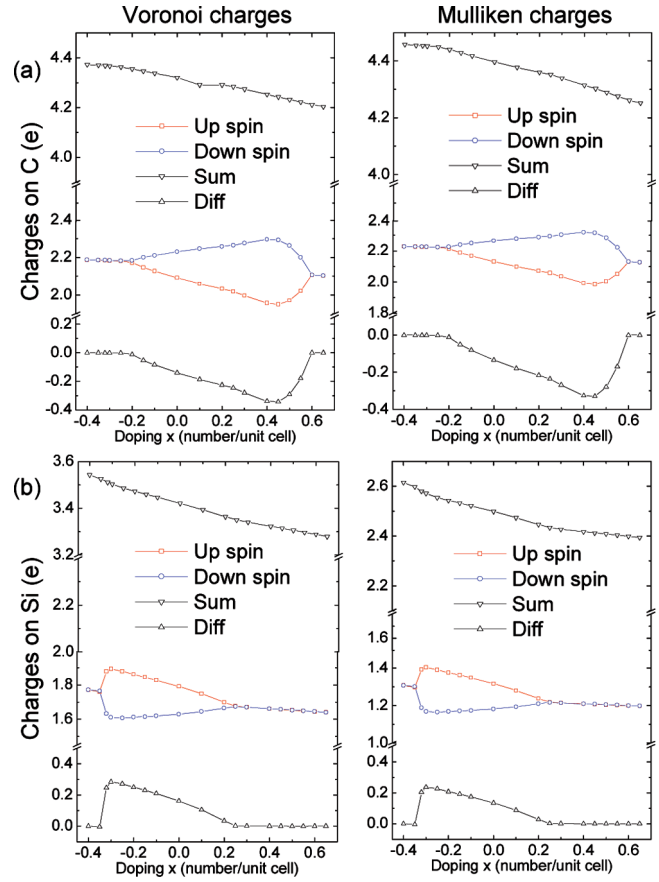

Figure 5. Voronoi and Mulliken charges on the (a) edge C atoms and (b) edge Si atoms of 4-ZSiC NR in the ground state with x electrons added or removed per unit cell ($x = 0$ for undoping, $x < 0$ for electron doping, and $x > 0$ for hole doping).

the charge in the spin-up channel ($Q_{Si}^{\uparrow}$) decreases. As a result, the local magnetic moment at the edge Si atoms decreases. At $x \simeq 0.25$, the charges in both the spin-up and spin-down channels ($Q_{Si}^{\uparrow}$ and $Q_{Si}^{\downarrow}$) are equal, and the local magnetic moment at the edge Si atoms disappears.

In contrast, the electron doping gives opposite behaviors. For the edge C atoms, the charge in the spin-down channel ($Q_C^{\downarrow}$) decreases slowly with electron doping, while the charge in the spin-up channel ($Q_C^{\uparrow}$) increases. As a result, the local magnetic moment at the edge C atoms is weakened. At $x \simeq -0.2$, the charges in both the spin-up and spin-down channels ($Q_C^{\uparrow}$ and $Q_C^{\downarrow}$) are equal, and the local magnetic moment at the edge C atoms disappears. For the edge Si atoms, the charge in the spin-down channel ($Q_{Si}^{\downarrow}$) decreases slowly with electron doping, while the charge in the spin-up channel ($Q_{Si}^{\uparrow}$) increases. As a result, the local magnetic moment at the edge Si atoms increases. After $x \simeq -0.3$, the charge in the spin-down channel ($Q_{Si}^{\downarrow}$) turns to increase with the electron doping, while the charge in the spin-up channel ($Q_{Si}^{\uparrow}$) turns to decrease. As a result, the local magnetic moment at the edge Si atoms turns to decrease. At $x \simeq -0.35$, the charges in both the spin-up and spin-down channels ($Q_{Si}^{\uparrow}$ and $Q_{Si}^{\downarrow}$) are equal, and the local magnetic moment at the edge Si atoms disappears.

We know that the above-mentioned carrier doping was usually performed in the real system by the field effect transistor (FET) doping technique. However, what about chemical doping? It is known that the electronic configuration of the ground of the C atom is $1s^2 2s^2 2p^2$, the nitrogen (N) atom is $1s^2 2s^2 2p^3$, and the boron (B) atom is $1s^2 2s^2 2p^1$. Thus, the substitution of the C

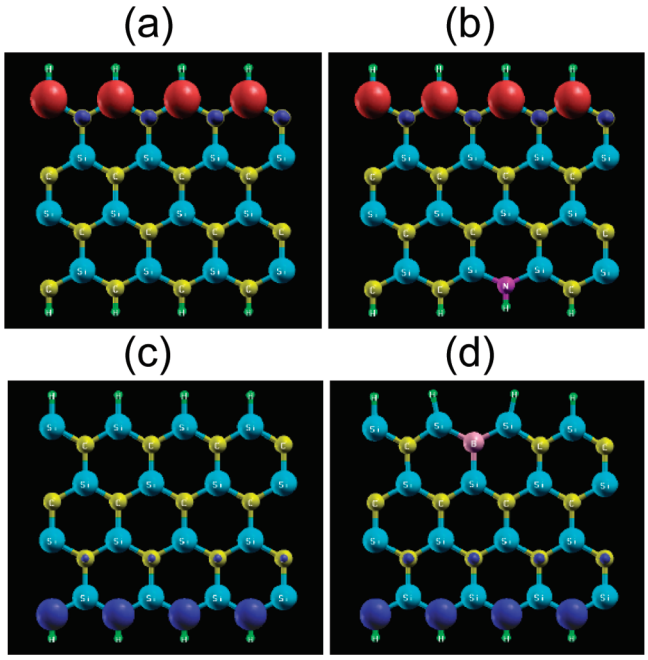

Figure 6. Spatial distribution of the spin differences of 4-ZSiC NR: (a, b) for electron doping and (c, d) for hole doping. One of the edge C atoms in panels b and d has been replaced by N and B atoms, respectively, which are shown in different colors. For the spatial distribution of the spin differences, the red and blue surfaces represent the spin-up and spin-down, which was drawn by the XCrySDen (Crystalline Structures and Densities) program.[56]

TABLE 1: Magnetic Moments (M) in Each Super Cell and Local Magnetic Moments at the Edge Atoms (M_x) of the Ground State for the 4-ZSiC NR

	$x = -0.25$	N-doped	$x = 0.25$	B-doped
M (μ_B)	0.99923	0.99925	−1.00091	−0.99982
M_C (μ_B)	−0.00105	−0.00086	−0.22878	−0.21945
M_{Si} (μ_B)	0.22809	0.22402	0.00082	0.00039

atoms by N atoms (called as N doping) brings the electron carrier, while substitution by B atoms (B doping) brings the hole carrier. Therefore, we study the cases of substitutions of B and N. To investigate the chemical doping effect in the 4-ZSiC NR, we introduce single B and N atoms in each super cell that includes 40 host atom sites (see Figure 6b,d), and this doping corresponds to the case $|x| = 0.25$ number/unit. We optimized the geometry and find that the substituted atoms are located in the ZSiC NR plane. The calculated magnetic moments (M) in each super cell and local magnetic moments at the edge atoms (M_x) of the ground state for the 4-ZSiC NR are given in Table 1. The corresponding spatial distribution of the spin differences is shown in Figure 6. It is found that the magnetic moments (M) in each super cell, as well as local magnetic moments at the edge C atoms (M_C) and the edge Si atoms (M_{Si}), for the N-doped and B-doped cases, are similar to the electron and hole doping, respectively.

It should be mentioned that here we only analyzed the case of 4-ZSiC NR. However, the general case of N-ZSiC NR is similar to the case of 4-ZSiC NR (Supporting Information), except that the critical values of x_e^{up}, x_e^{down}, x_h^{up}, and x_h^{down} depend on the width of N-ZSiC NR. On the other hand, we also have studied the band structures of 4-ZSiC NR in the ground state with electron doping ($x = -0.25$), without doping ($x = 0$), and with hole doping ($x = 0.25$) using the projector augmented wave (PAW)[57,58] method for the electron-ion interaction with PBE exchange correlation functionals, as implemented in the Quantum-ESPRESSO package.[59] It is clearly shown that the behavior of the magnetization and change of the magnetization direction of the ZSiC NRs controlled by carrier (hole and electron) doping is independent of the treatment method of the electron-ion interaction even though the different treatments of the electron-ion interaction may lead to the quantitative difference in band structures (see Figures S1 and S2 in the Supporting Information). This indicates that the behavior of the magnetization and change of the magnetization direction of the ZSiC NRs controlled by carrier (hole and electron) is the intrinsic physical behavior of the system.

It is noted that in the case of graphene nanoribbons there are many factors that can affect the presence of the ferromagnetism of the edges. For example, Koskinen, Malola, and Häkkinen found that the zigzag edge is metastable and a planar reconstruction spontaneously takes place at room temperature.[60] Boukhvalov and Katsnelson found that the magnetic state of edges in graphene nanoribbons may be unstable, with respect to oxidation and water dissociation at the edges.[61] Moreover, Yazyev and Katsnelson have shown that the perfect order of the ferromagnetism of the edges is strongly affected by thermal excitations, thus imposing strict limitations on graphene nanoribbons for spintronic devices.[62] It is expected that some similar factors exist for spintronics devices based on ZSiC NRs. Nevertheless, the magnetic zigzag edges of ZSiC NRs would be a good candidate for novel spintronics devices despite the fact that no true long-range magnetic order is possible in one dimension. In other words, we assumed that the magnetic interaction along the edge lines was FM and neglected the formation of a spin domain wall, i.e., we assumed that the length of the ribbon edges used in devices was smaller than the length of the magnetic order of zigzag edges of ZSiC NRs.

Conclusions

It is found that the magnetic properties of the ZSiC NRs are shown to be tunable by electron, hole, and chemical doping. The chemical doping by nitrogen and boron atoms gave similar results with the electron and hole doping, respectively. The ZSiC NRs can be *magnetized* by the doping, and the magnetization direction can be modulated. These findings open up a new route toward doping control of magnetization, which may lead to some important applications of the ZSiC NRs in spintronics, such as switches and sensors.

Acknowledgment. This work was supported by the National Research Foundation (NRF) Grant funded by the Korean Government (MEST) (R11-2007-012-03002-0) (2009). This work was also supported by the Postdoctoral Research Program of Sungkyunkwan University (2008).

Supporting Information Available: Computational details and the results of the PWSCF code of Quantum ESPRESSO, band structures of N-ZSiC NRs ($N = 4$, 5, 6, 7, 8, and 10) with and without doping, as well as plots of the total energy and Fermi energy of 4-ZSiC NR in the ground state with electron doping ($x = -0.25$), without doping ($x = 0$), and hole doping ($x = 0.25$) as a function of the number of k-point sampling in the Brillouin zone integration. This material is available free of charge via the Internet at http://pubs.acs.org.

References and Notes

(1) Žutić, I.; Fabian, J.; Das Sarma, S. *Rev. Mod. Phys.* **2004**, *76*, 323.
(2) (a) Kim, W. Y.; Kim, K. S. *Nat. Nanotechnol.* **2008**, *3*, 408. (b) Kim, W. Y.; Choi, Y. C.; Min, S. K.; Cho, Y. C.; Kim, K. S. *Chem. Soc.*

Rev. **2009**, *38*, 2319. (c) Kim, W. Y.; Choi, Y. C.; Kim, K. S. *J. Mater. Chem.* **2008**, *18*, 4510.
(3) Guo, J.; Gunlycke, D.; White, C. T. *Appl. Phys. Lett.* **2008**, *92*, 163109.
(4) Muñoz-Rojas, F.; Fernández-Rossier, J.; Palacios, J. J. *Phys. Rev. Lett.* **2009**, *102*, 136810.
(5) León, A.; Barticevic, Z.; Pacheco, M. *Appl. Phys. Lett.* **2009**, *94*, 173111.
(6) Zheng, X. H.; Wang, R. N.; Song, L. L.; Dai, Z. X.; Wang, X. L.; Zeng, Z. *Appl. Phys. Lett.* **2009**, *95*, 123109.
(7) Nguyen, V. H.; Do, V. N.; Bournel, A.; Nguyen, V. L.; Dollfus, P. *J. Appl. Phys.* **2009**, *106*, 053710.
(8) Castro Neto, A.; Guinea, F.; Peres, N.; Novoselov, K.; Geim, A. *Rev. Mod. Phys.* **2009**, *81*, 109.
(9) Han, M. Y.; Ozyilmaz, B.; Zhang, Y.; Kim, P. *Phys. Rev. Lett.* **2007**, *98*, 206805.
(10) Berger, C.; Song, Z.; Li, X.; Wu, X.; Brown, N.; Naud, C.; Mayou, D.; Li, T.; Hass, J.; Marchenkov, A. N.; Conrad, E. H.; First, P. N.; Heer, W. A. d. *Science* **2006**, *312*, 1191.
(11) Ci, L.; Xu, Z.; Wang, L.; Gao, W.; Ding, F.; Kelly, K.; Yakobson, B. I.; Ajayan, P. *Nano Res.* **2008**, *1*, 116.
(12) Chen, Z.; Lin, Y.; Rooks, M. J.; Avouris, P. *Phys. E* **2007**, *40*, 228.
(13) Cancado, L. G.; Pimenta, M. A.; Neves, B. R. A.; Medeiros-Ribeiro, G.; Enoki, T.; Kobayashi, Y.; Takai, K.; Fukui, K.; Dresselhaus, M. S.; Saito, R.; Jorio, A. *Phys. Rev. Lett.* **2004**, *93*, 047403.
(14) Lee, H.; Son, Y. W.; Park, N.; Han, S.; Yu, J. *Phys. Rev. B* **2005**, *72*, 174431.
(15) Ezawa, M. *Phys. Rev. B* **2006**, *73*, 045432.
(16) Son, Y. W.; Cohen, M. L.; Louie, S. G. *Phys. Rev. Lett.* **2006**, *97*, 216803.
(17) Ezawa, M. *Phys. Rev. B* **2007**, *76*, 245415.
(18) Ezawa, M. *Phys. E* **2008**, *40*, 1421.
(19) Son, Y. W.; Cohen, M. L.; Louie, S. G. *Nature (London)* **2006**, *444*, 347.
(20) Hod, O.; Barone, V.; Peralta, J. E.; Scueria, G. E. *Nano Lett.* **2007**, *7*, 2295.
(21) Kan, E. J.; Li, Z.; Yang, J.; Hou, J. G. *Appl. Phys. Lett.* **2007**, *91*, 243116.
(22) Hod, O.; Barone, V.; Scuseria, G. E. *Phys. Rev. B* **2008**, *77*, 035411.
(23) Fujita, M.; Wakabayashi, K.; Nakada, K.; Kusakabe, K. *J. Phys. Soc. Jpn.* **1996**, *65*, 1920.
(24) Wakabayashi, K.; Fujita, M.; Ajiki, H.; Sigrist, M. *Phys. Rev. B* **1999**, *59*, 8271.
(25) Barone, V.; Hod, O.; Scuseria, G. E. *Nano Lett.* **2006**, *6*, 2748.
(26) Kudin, K. N. *ACS Nano* **2008**, *2*, 516.
(27) Sawada, K.; Ishii, F.; Saito, M. *Appl. Phys. Express* **2008**, *1*, 064004.
(28) Sawada, K.; Ishii, F.; Saito, M.; Kawai, T. *Nano Lett.* **2009**, *9*, 269.
(29) Sergio, D. D.; Zachary, H. L. *J. Phys. Chem. C* **2008**, *112*, 8196.
(30) Zhang, X. W.; Yang, G. W. *J. Phys. Chem. C* **2009**, *113*, 4662.
(31) Li, Y.; Zhou, Z.; Shen, P.; Chen, Z. *J. Phys. Chem. C* **2009**, *113*, 15043.
(32) Sharma, R.; Nair, N.; Strano, M. S. *J. Phys. Chem. C* **2009**, *113*, 14771.
(33) Lu, Y. H.; Feng, Y. P. *J. Phys. Chem. C* **2009**, *113*, 20841.
(34) Li, Y.; Zhou, Z.; Shen, P.; Chen, Z. *ACS Nano* **2009**, *3*, 1952.
(35) Nduwimana, A.; Wang, X. Q. *ACS Nano* **2009**, *3*, 1995.
(36) Kinder, J. M.; Dorando, J. J.; Wang, H.; Chan, G. K. L. *Nano Lett.* **2009**, *9*, 1980.
(37) Hod, O.; Scuseria, G. E. *Nano Lett.* **2009**, *9*, 2619.
(38) Biel, B.; Triozon, F.; Blase, X.; Roche, S. *Nano Lett.* **2009**, *9*, 2725.
(39) Cantele, G.; Lee, Y. S.; Ninno, D.; Marzari, N. *Nano Lett.* **2009**, *9*, 3425.
(40) Lee, H.; Ihm, J.; Cohen, M. L.; Louie, S. G. *Nano Lett.* **2010**, *10*, 793.
(41) Kim, W. Y.; Kim, K. S. *Acc. Chem. Res.* **2010**, *43*, 111.
(42) Wassmann, T.; Seitsonen, A. P.; Saitta, A. M.; Lazzeri, M.; Mauri, F. *J. Am. Chem. Soc.* **2010**, *132*, 3440.
(43) Zheng, X. H.; Wang, X. L.; Abtew, T. A.; Zeng, Z. *J. Phys. Chem. C* **2010**, *114*, 4190.
(44) Wu, M.; Wu, X.; Zeng, X. C. *J. Phys. Chem. C* **2010**, *114*, 3937.
(45) Lee, Y. L.; Kim, S.; Park, C.; Ihm, J.; Son, Y. W. *ACS Nano*, **2010**, *4*, 1345.
(46) Lottermoser, T.; Lonkai, T.; Amann, U.; Hohlwein, D.; Ihringer, J.; Fiebig, M. *Nature (London)* **2004**, *430*, 541.
(47) Eerenstein, W.; Wiora, M.; Prieto, J. L.; Mathur, N. D.; Scott, J. F. *Nat. Mater.* **2007**, *6*, 348.
(48) Lou, P.; Lee, J. Y. *J. Phys. Chem. C* **2009**, *113*, 21213.
(49) Lou, P.; Lee, J. Y. *J. Phys. Chem. C* **2009**, *113*, 12637.
(50) OpenMX Website: Ozaki, T.; Kino, H.; Yu, J.; Han, M. J.; Kobayashi, N.; Ohfuti, M.; Ishii, F.; Ohwaki, T.; Weng, H. http://www.openmx-square.org/.
(51) Perdew, J. P.; Burke, K.; Ernzerhof, M. *Phys. Rev. Lett.* **1996**, *77*, 3865.
(52) Troullier, N.; Martins, J. L. *Phys. Rev. B* **1991**, *43*, 1993.
(53) Ozaki, T. *Phys. Rev. B* **2003**, *67*, 155108.
(54) Ozaki, T.; Kino, H. *Phys. Rev. B* **2004**, *69*, 195113.
(55) Sun, L.; Li, Y.; Li, Z.; Li, Q.; Zhou, Z.; Chen, Z.; Yang, J.; Hou, J. G. *J. Chem. Phys.* **2008**, *129*, 174114.
(56) Kokalj, A. *Comput. Mater. Sci.* **2003**, *28*, 155.
(57) Blöchl, P. E. *Phys. Rev. B* **1994**, *50*, 17953.
(58) Kresse, G.; Joubert, D. *Phys. Rev. B* **1999**, *59*, 1758.
(59) Giannozzi, P.; Baroni, S.; Bonini, N.; Calandra, M.; Car, R.; Cavazzoni, C.; Ceresoli, D.; Chiarotti, G. L.; Cococcioni, M.; Dabo, I.; Dal Corso, A.; Fabris, S.; Fratesi, G.; de Gironcoli, S.; Gebauer, R.; Gerstmann, U.; Gougoussis, C.; Kokalj, A.; Lazzeri, M.; Martin-Samos, L.; Marzari, N.; Mauri, F.; Mazzarello, R.; Paolini, S.; Pasquarello, A.; Paulatto, L.; Sbraccia, C.; Scandolo, S.; Sclauzero, G.; Seitsonen, A. P.; Smogunov, A.; Umari, P.; Wentzcovitch, R. M. *J. Phys.: Condens. Matter* **2009**, *21*, 395502.
(60) Koskinen, P.; Malola, S.; Häkkinen, H. *Phys. Rev. Lett.* **2008**, *101*, 115502.
(61) Boukhvalov, D. W.; Katsnelson, M. I. *Nano Lett.* **2008**, *8*, 4373.
(62) Yazyev, O. V.; Katsnelson, M. I. *Phys. Rev. Lett.* **2008**, *100*, 047209.

JP911953Z